Chemical Physics Impact 2 (2021) 100017

Contents lists available at ScienceDirect

Chemical Physics Impact

journal homepage: www.elsevier.com/locate/chphi

The effect of swellable carboxymethyl cellulose coating on the physicochemical stability and release profile of a zinc hydroxide nitrate–sodium dodecylsulphate–imidacloprid

Sharifah Norain Mohd Sharif[a,*], Norhayati Hashim[a,b], Illyas Md Isa[a,b], Suriani Abu Bakar[c], Mohamad Idris Saidin[a], Mohamad Syahrizal Ahmad[a], Mazidah Mamat[d], Mohd Zobir Hussein[e], Rahadian Zainul[f], Azlan Kamari[a]

[a] *Department of Chemistry, Faculty of Science and Mathematics, Universiti Pendidikan Sultan Idris, 35900 Tanjong Malim, Perak, Malaysia*
[b] *Nanotechnology Research Centre, Faculty of Science and Mathematics, Universiti Pendidikan Sultan Idris, 35900 Tanjong Malim, Perak, Malaysia*
[c] *Department of Physics, Faculty of Science and Mathematics, Universiti Pendidikan Sultan Idris, 35900 Tanjong Malim, Perak, Malaysia*
[d] *Faculty of Science and Environment Marine, Universiti Malaysia Terengganu, 21030 Kuala Terengganu, Terengganu, Malaysia*
[e] *Materials Synthesis and Characterization Laboratory, Institute of Advanced Technology, Universiti Putra Malaysia, 43400 Serdang, Selangor, Malaysia*
[f] *Department of Chemistry, Faculty of Mathematics and Natural Science, Universitas Negeri Padang, West Sumatera 25171, Indonesia*

ARTICLE INFO

Keywords:
Carboxymethyl cellulose
Zinc hydroxide nitrate
Sodium dodecylsulphate
Imidacloprid
Controlled release properties

ABSTRACT

The environmental pollution that results from the excessive usage of pesticides has been threatening the communities for decades. In this study, carboxymethyl cellulose (CMC) is proposed as a coating agent to encapsulate zinc hydroxide nitrate–sodium dodecylsulphate–imidacloprid (ZHN–SDS–IC) for the implementation of controlled release formulation (CRF) in pesticide. The physicochemical properties of the ZHN–SDS–IC–CMC were characterised so that their crystallinity, thermal behaviour and surface morphology could be examined. The findings from the release study revealed the potential for CMC to prolong the release of imidacloprid (IC). A strong hygroscopic and adequate swelling characteristic enabled the CMC to develop an external gel layer on the surface of the ZHN–SDS–IC–CMC that acted as an additional barrier and slowed the release of the intercalated IC. The ZHN–SDS–IC–CMC that was synthesised can contribute to overcoming the environmental issues due to excessive usage of pesticides and can create a better future for the community.

Introduction

Imidacloprid (IC) is a systemic soil and foliar insecticide that is frequently used to protect paddy cultivation areas from the threats of aphids, plant bugs, leafhoppers, planthoppers and other invasive pests [1]. It is classified as a neonicotinoid insecticide, which acts by disturbing the nicotinic acetylcholine receptors in the central nervous systems of the targeted pests [2]. Although the uses of IC may be beneficial to the paddy cultivation sector, the excessive and uncontrollable use of IC could cause water and soil pollution.

Hence, considerable effort has been expended to explore the controlled release formulation (CRF) approach in the agricultural sector [3–8]. The development of CRF in pesticides could be very convenient for the commercial formulations, since the CRF offers several interesting benefits, including the continuation of a low amount pesticide release over period of time. It is also more economical, environmental friendly and can reduce the application frequency of the pesticide [9]. The pesticide with CRF properties can ameliorate pesticide residues as well as those by leaching, evaporation and degradation, hence minimising the negative impact on the environment [1].

In recent years, clay-based host materials, have provoked extensive interest as a means to control the release of pesticide into the environment [10,11]. These materials were reported to be exploited not only in agricultural field, but also in numerous other fields, including medicinal, cosmetic, food technology and sensor development [12–17]. Due to its simple preparation and good ion exchange properties, the clay-based host materials, such as zinc hydroxide nitrate, $Zn_5(OH)_8(NO_3)_2.2H_2O$

Abbreviations: IC, imidacloprid; CRF, controlled release formulation; CMC, carboxymethyl cellulose; ZHN–SDS, zinc hydroxide nitrate–sodium dodecylsulphate; ZHN–SDS–IC, zinc hydroxide nitrate–sodium dodecylsulphate–imidacloprid; ZHN–SDS–IC–CMC, zinc hydroxide nitrate–sodium dodecylsulphate–imidacloprid–carboxymethyl cellulose; PXRD, Powder X-ray diffraction; FTIR, Fourier-transform infrared; TGA/DTG, thermogravimetric analysis and derivative thermogravimetric analysis; FESEM, field emission scanning electron microscopy; UV/Vis, ultraviolet visible.

* Corresponding author.
E-mail address: norain.sharif@fsmt.upsi.edu.my (S.N.M. Sharif).

https://doi.org/10.1016/j.chphi.2021.100017
Received 7 November 2020; Received in revised form 20 February 2021; Accepted 7 March 2021

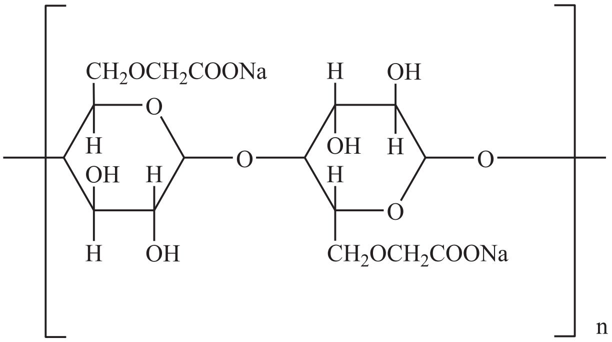

Fig. 1. The chemical structure of carboxymethyl cellulose (CMC).

or ZHN, has been used as a host material for numerous nanocomposites by intercalated them with a wide range of ions, such as 3-(4-methoxyphenyl)propionic acid, azelate, metalloporphyrins, adipate and benzoate [18–20]. In some cases, surfactants like sodium dodecyl sulphate (SDS), polyoxyethylene(10)nonyl phenyl ether (TX–10) and dodecyl betaine dodecylbenzenesulfonate (DBS) were also purposely added into the mixture during synthesis phase, in order to assist the intercalation process [21,22]. This method is particularly useful in the intricate intercalation process, involving neutrally charged and poorly water soluble pesticides. The ability of surfactants in minimizing surface tension, altering energy relationships at the interface, forming micelle and creating a hydrophobic region in the interlayer gallery of the layered material, is therefore, contribute in creating a conducive environment for the intercalation process [23].

Through the surface modification with polymers, it is possible to further improve the CRF properties of the clay-based nanocomposite. Recent studies reported on the encapsulation approach using a cellulose derivative, carboxymethyl cellulose (CMC), to generate the formation of a gel layer on the outer surface of the nanocomposite, which helps to prolong the time release of the pesticide [24]. Due to the biodegradability and non-toxic nature of CMC, this cellulose derivative seems to be an excellent material for use as a coating material to develop a safer and greener pesticide [25,26]. The water absorbency and gel content properties owned by CMC not only allowing them to be used for CRF in zinc micronutrient fertilizer systems but also in the fabrication of CMC hydrogel beads for biomaterial applications [27,28]. The carboxyl and hydroxyl groups that were found in the CMC structure activated its gelation forming ability and formed the hydrogel layer. Gelatin, κ-carrageenan, chitosan, poly(acrylamide-co-itaconic acid), poly(acrylic acid-co-itaconic acid), poly(vinyl alcohol), poly(acrylic acid) and poly(acrylamide) are some of the examples of hydrogel that were also exploited for their gelation forming ability [27–34]. The chemical structure of the CMC is shown in Fig. 1.

The present study aimed to develop a pesticide with better CRF properties by encapsulating the zinc hydroxide nitrate–sodium dodecylsulphate-imidacloprid (ZHN–SDS–IC) nanocomposite with CMC. For this purpose, characterization studies were performed using several analytical techniques to investigate the physicochemical properties after the ZHN–SDS–IC nanocomposite underwent the CMC coating process (the coated nanocomposite is referred as ZHN–SDS–IC–CMC). The release study of the ZHN–SDS–IC–CMC was carried out in few sets of aqueous solutions, and the release data were fitted with several kinetic models so that its release mechanism could be determined.

Experimental

Materials

Most of the reagents used in this study were purchased from Systerm, Merck and Sigma Aldrich. Zinc nitrate ($Zn(NO_3)_2.6H_2O$) with a purity of 98% was supplied by Systerm and IC (98% purity) was obtained from Essense (China). Hydrochloric acid (HCl) was purchased from Merck and the sodium hydroxide (NaOH) was obtained from Sigma Aldrich. Surfactants SDS and the CMC were obtained from Systerm and Sigma Aldrich, respectively. The aqueous solutions that were used as release media were prepared using sodium phosphate (Na_3PO_4) with a purity of 99.5% and were supplied by Merck. The sodium sulphate (Na_2SO_4) with a purity of 95.2% and sodium chloride (NaCl) with a purity of 99.0% were obtained from Systerm. No further purification was performed on any of the reagents before they were used, and deionised water was used to prepare all solutions needed in the study.

Synthesis of ZHN–SDS, ZHN–SDS–CMC, ZHN–SDS–IC and ZHN–SDS–IC–CMC nanocomposite

The procedure to synthesize the ZHN–SDS and ZHN–SDS–IC nanocomposites have been described in detail in a paper recently published by the author [35]. Briefly, the ZHN–SDS was synthesised using a co-precipitation method in a pH controlled environment (pH 6.5) that used $Zn(NO_3)_2.6H_2O$ and SDS as precursors. The pH was adjusted by the dropwise addition of HCl and NaOH. The ZHN–SDS–IC nanocomposite was synthesised by dispersing the ZHN–SDS in an IC solution and stirred at room temperature (2 h). The mixture was aged in an oil bath shaker at 70 °C (24 h) and then centrifuged at 4000 rpm (5 min) and dried in an oven (24 h). The percentage loading of IC intercalated in the interlayer gallery of ZHN–SDS–IC have been determined and reported in our previously published paper, which is 40.88% [35].

The ZHN–SDS was coated using CMC with a ZHN–SDS:CMC mass ratio of 1:1. A quantity of 0.1 g CMC was weighed and dissolved using 50 mL deionised water as the solvent. The CMC solution was continuously stirred at room temperature until the CMC was completely dissolved. Then 0.1 g ZHN–SDS was added into the mixture and constantly stirred at room temperature for 18 h to ensure the completion of the CMC coating process. The mixture was centrifuged (at 4000 rpm for 5 min), dried in an oven and ground into fine powder before it was stored in sample bottle. The final product was denoted as ZHN–SDS–CMC. Similar procedures for the coating process were performed on the ZHN–SDS–IC nanocomposite, and that product was denoted as the ZHN–SDS–IC–CMC nanocomposite.

Sample characterization

Several instrumentations were used to investigate the physicochemical properties of the ZHN–SDS–CMC and ZHN–SDS–IC–CMC. Powder X-ray diffraction (PXRD) measurements were performed on a PANalytical X-pert Pro MPD diffractometer using Co K-alpha radiation (k=0.15406 nm) at 30 mA and 40 kV. The scan range was 2°–60° 2θ, with an increment of 2°/min, a step size of 0.0330° and scan step time of 19.4434 s. The Fourier-transform infrared (FTIR) measurements were performed using the KBr disk technique on a Nicolet FTIR spectrometer. The transmission mode for the scanning was from 400 to 4000 cm^{-1} with a nominal resolution of 4 cm^{-1}. The thermal degradation behaviour of the samples was studied using thermogravimetric analysis and derivative thermogravimetric analysis (TGA/DTG) on a Perkin-Elmer Pyris 1 TGA Thermo Balance and was performed under a nitrogen atmosphere. The temperature was increased from room temperature to 1000 °C at a heating rate of 10 °C min^{-1}. The surface morphology analysis was examined using field emission scanning electron microscopy (FESEM) with a Hitachi SU 8020 UHR instrument at 5.0 kV and 10 k magnification.

Controlled release formulation study of the ZHN–SDS–IC–CMC nanocomposite

The release of IC from the interlayer gallery of ZHN–SDS–IC–CMC was investigated in aqueous solutions of Na_3PO_4, Na_2SO_4 and NaCl.

The aqueous solutions for the single system were prepared in a series of concentrations (0.1 M, 0.3 M and 0.5 M) whereas the binary and ternary system were prepared in 0.5 M aqueous solutions of several combination (PO_4^{3-}–SO_4^{2-}, PO_4^{3-}–Cl^- and SO_4^{2-}–Cl^- and PO_4^{3-}–SO_4^{2-}–Cl^-). This release experiments were carried out using a Lambda 25 Perkin Elmer ultraviolet visible (UV/Vis) spectrometer, with the lambda max value of 269.5 nm. In every measurement, 0.6 mg of the ZHN–SDS–IC–CMC was released in a quartz cuvette containing 3.5 mL of the aqueous solutions. The cuvette was left in the UV/Vis spectrometer for several days, until the release study was completed. The maximum absorbance values were converted into ppm, and the percentage accumulated release of the IC in each release media was determined. The experimental conditions for the measurement were as follows: the time interval was 60 s, slit width was 1.0 nm, lamp change was 326.0 nm, ordinate max was 1.0 and the ordinate min was 0.0.

Results and discussion

PXRD analysis

The ZHN–SDS and ZHN–SDS–IC nanocomposites were coated using CMC and the resulting products were characterised by PXRD, as shown in Fig. 2. The PXRD analysis examined the crystallinity of the nanocomposite and determined any changes in the basal spacing of the nanocomposites. Generally, the analysis of the PXRD patterns revealed that the CMC coating process brought about a slight transformation for both the ZHN–SDS and ZHN–SDS–IC nanocomposites.

In the PXRD pattern for the ZHN–SDS–CMC, a clear decrease of the intensity for each diffraction peak can be clearly observed, which indicated that the CMC coating process led to the formation of weaker diffraction peaks. The presence of the amorphous CMC structure in the ZHN–SDS–CMC affected its crystallinity and lowered the intensity of the peaks. The diffraction peaks in the PXRD pattern for the ZHN–SDS–CMC (with a basal spacing of 33.0 Å, 10.0 Å and 4.9 Å) were comparable to the PXRD pattern of ZHN–SDS (with a basal spacing of 33.0 Å, 9.8 Å and 4.9 Å). This indicated that there was not a significant change in the height of the interlayer gallery of the ZHN–SDS–CMC. This confirmed that the CMC coating process on the ZHN–SDS preserved the intercalation of the SDS in its interlayer gallery.

The diffraction peaks for the ZHN–SDS–IC nanocomposite demonstrated the common features for a crystalline layered material, which are intense, sharp and symmetrical peaks. The peaks appeared at low 2θ angle and indicated a basal spacing of 32.0 Å, 16.3 Å and 10.9 Å. After the ZHN–SDS–IC underwent the CMC coating process, the peaks in the PXRD pattern generally resembled the peaks in the PXRD pattern for the ZHN–SDS–IC nanocomposite. However, those peaks were slightly shifted and appeared with a basal spacing of 33.4 Å, 16.4 Å and 11.0 Å. The peaks that indicated a turbostratic effect were observed in the PXRD pattern for both ZHN–SDS–IC and ZHN–SDS–IC–CMC nanocomposites in the 2θ range from 32.1° to 35.5°. This was caused by the decrease in the order along the stacking axis. The appearance of the comparable peaks in both PXRD patterns indicated that the CMC did not cause any alteration on the stacking axis of the nanocomposite. The peaks in the PXRD pattern for ZHN–SDS–IC–CMC also had a lower intensity and broader shape due to the amorphous nature of the CMC coated on its surface. There was an insignificant difference in the basal spacing before and after the coating process, which indicated that the ions that were intercalated in the interlayer gallery of ZHN–SDS–IC were not replaced.

The results from the PXRD analysis revealed that the ZHN–SDS–IC–CMC behaved in the same way as in the PXRD pattern for the ZHN–SDS–CMC. The basal spacing of the diffraction peaks before and after the CMC coating was very similar due to the fact that the additional CMC was only adsorbed on the surface of ZHN–SDS and ZHN–SDS–IC and was not exchanged with the intercalated ions. A comparable behaviour was also reported in recent studies [36,37].

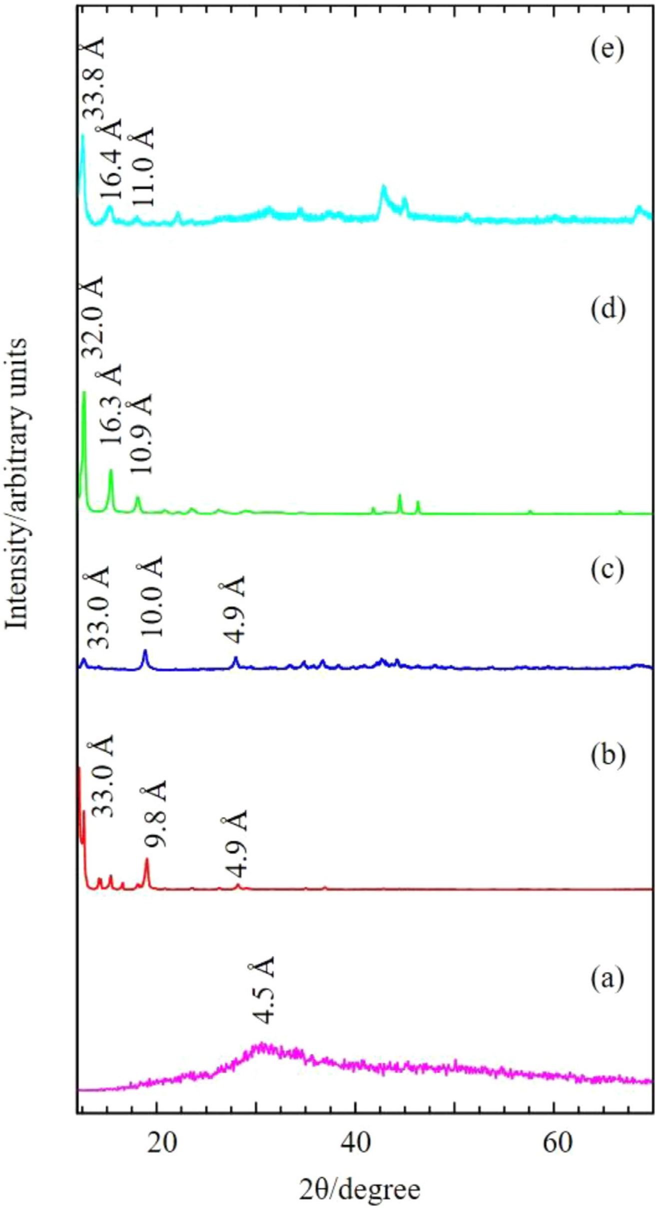

Fig. 2. PXRD patterns of (a) carboxymethyl cellulose, (b) ZHN–SDS, (c) ZHN–SDS–CMC, (d) ZHN–SDS–IC [35] and (e) ZHN–SDS–IC–CMC.

Spatial arrangement of carboxymethyl cellulose coated ZHN–SDS–IC nanocomposite

The spatial arrangement of the IC and SDS within the interlayer gallery of the ZHN–SDS–IC and ZHN–SDS–IC–CMC was predicted using Chem 3D Ultra 8.0 software, and is illustrated in Fig. 3. The molecular size of both the IC and SDS were found to be 12.5 × 9.2 × 7.2 Å and 19.9 × 6.1 × 5.2 Å, respectively. Based on the result obtained from the PXRD analysis, the basal spacing of the ZHN–SDS–IC was determined to be 32.0 Å. The ZHN was made up of an inorganic layer with octahedral coordinated Zn^{2+}, and one quarter of the octahedral were vacant. The tetrahedral coordinated Zn^{2+} was positioned below and above the octahedral layer [38]. Considering the thickness of ZHN layer was 4.8 Å and the thickness of Zn tetrahedron was 2.6 Å, the interlayer gallery height was calculated to be 22.0 Å. Therefore, both SDS and IC were intercalated in the interlayer gallery of ZHN–SDS–IC in a vertical monolayer arrangement.

Table 1
FTIR spectra of ZHN–SDS, IC, ZHN–SDS–IC, carboxymethyl cellulose, ZHN–SDS–CMC and ZHN–SDS–IC–CMC.

Characteristic Group	ZHN–SDS	Imidacloprid	ZHN–SDS–IC	Carboxy-methyl cellulose	ZHN–SDS–CMC	ZHN–SDS–IC–CMC
v (O–H) in H_2O	3458	–	3492	3512	3468	3528
v_s (C–O–C) in CMC	–	–	–	1051	1057	1053
v_{as} (S=O) in SDS	1217	–	960	–	1210	1203
v_s (S–O) in SDS	827	–	751	–	834	820
v_s (C–H) in SDS	2840	–	2938	–	2849	2851
	2920				2916	2917
	2957				2960	2959
v_s (COO^-) in CMC	–	–	–	1618	1622	1616
v_{as} (COO^-) in CMC	–	–	–	1432	1370	1392
Pyridine in IC	–	1559	1609	–	–	1575
v_s (N–O) in IC	–	1388	1431	–	–	1479
Ref.	[35]	[35]	[35]	Present paper	Present paper	Present paper

Abbreviation: ZHN–SDS, zinc hydroxide nitrate–sodium dodecylsulphate; ZHN–SDS–IC, zinc hydroxide nitrate–sodium dodecylsulphate–imidacloprid; ZHN–SDS–CMC, zinc hydroxide nitrate–sodium dodecylsulphate–carboxymethyl cellulose; ZHN–SDS–IC–CMC, zinc hydroxide nitrate–sodium dodecylsulphate–imidacloprid–carboxymethyl cellulose.

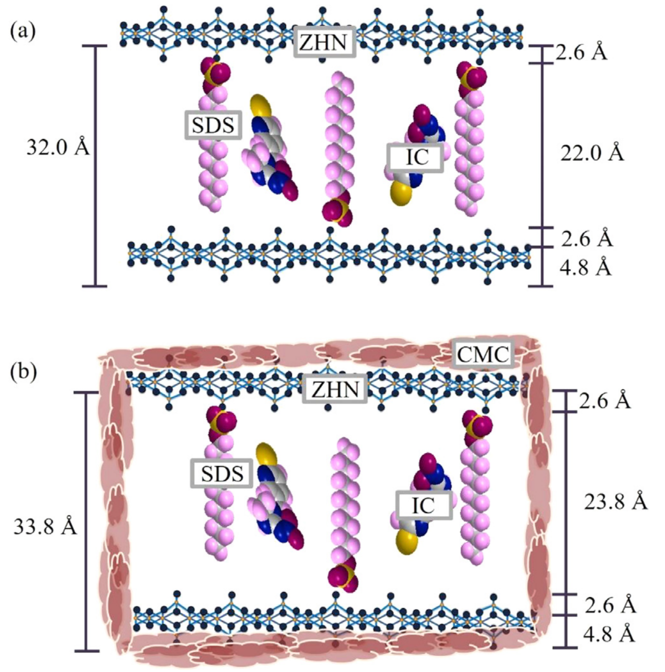

Fig. 3. The proposed spatial orientation of IC and SDS in the interlayer gallery of (a) ZHN–SDS–IC-and (b) ZHN–SDS–IC–CMC.

For the case of ZHN–SDS–IC–CMC, a slight increase in the basal spacing was observed after the nanocomposite underwent the CMC coating process, which happened to be 33.8 Å. A similar calculation was made by deducting the value of the basal spacing with the thickness of the ZHN and Zn tetrahedron. After the deduction, the free interlayer gallery was found to be 23.8 Å, which was greater than in the interlayer gallery of the ZHN–SDS–IC nanocomposite. The spacious interlayer gallery allowed the ZHN–SDS–IC–CMC to preserve the vertical monolayer arrangement, as for the ZHN–SDS–IC.

FTIR analysis

The FTIR analysis was performed to monitor any changes in the functional group of the ZHN–SDS and ZHN–SDS–IC nanocomposite after the CMC coating process. The FTIR spectra of the prepared materials are shown in Fig. 4. The results were also compared with the FTIR pattern of the uncoated ZHN–SDS and ZHN–SDS–IC reported in our previous study and summarised into Table 1. The peaks that indicate the

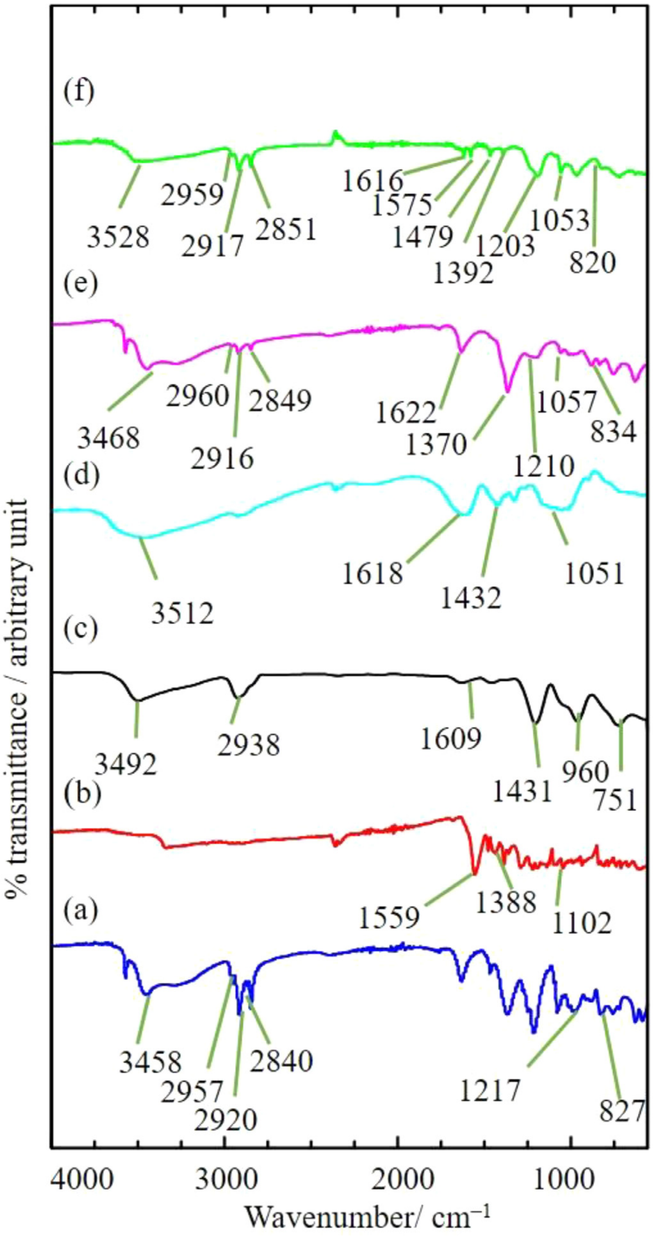

Fig. 4. FTIR spectra (a) ZHN–SDS [35], (b) IC anion [35], (c) ZHN–SDS–IC [35], (d) carboxymethyl cellulose, (e) ZHN–SDS–CMC and (f) ZHN–SDS–IC–CMC.

stretching of the hydroxyl group can be seen in the FTIR spectra of ZHN–SDS, CMC, ZHN–SDS–CMC, ZHN–SDS–IC and ZHN–SDS–IC–CMC at 3458 cm^{-1}, 3512 cm^{-1}, 3468 cm^{-1}, 3492 cm^{-1}and 3528 cm^{-1}, respectively [21].

In the FTIR spectra for ZHN–SDS and ZHN–SDS–CMC, the characteristic peaks for SDS can be seen in both spectra. The peaks that denote the C–H stretching and bending in the hydrophobic tail of the SDS were observed in the FTIR spectra of ZHN–SDS–CMC at 2960 cm^{-1}, 2916 cm^{-1} and 2849 cm^{-1} (and can also found in the FTIR spectra of ZHN–SDS at 2957 cm^{-1}, 2920 cm^{-1}, and 2840 cm^{-1}) [39,40]. The absorption peaks that signify the asymmetric stretching of S=O were observed in the FTIR spectra for ZHN–SDS at 1217 cm^{-1} and in the FTIR spectra of ZHN–SDS–CMC at 1210 cm^{-1}. The absorption peak for S–O stretching appeared in the FTIR spectra for ZHN–SDS and ZHN–SDS–CMC at 827 cm^{-1} and 834 cm^{-1}, respectively [22]. Additional peaks that indicate the presence of CMC were also observed in the FTIR spectra of ZHN–SDS–CMC at 1622 cm^{-1} and 1370 cm^{-1} due to the vibration of the symmetrical and asymmetrical stretching of the carboxylate group (originally found in the FTIR spectra of CMC at 1618 cm^{-1} and 1432 cm^{-1}, respectively) [41]. Another peak that was attributed to the –C–O– stretching on the polysaccharide skeleton of the CMC was observed in the FTIR spectra for ZHN–SDS–CMC at 1057 cm^{-1} (originally found in the FTIR spectra of CMC at 1051 cm^{-1}).

The characteristic peaks for the SDS and IC can be observed in the FTIR spectra for the ZHN–SDS–IC and ZHN–SDS–IC–CMC. The peaks that indicate C–H stretching and bending in the hydrocarbon backbone of SDS were observed in the FTIR spectra for ZHN–SDS–IC–CMC at 2959 cm^{-1}, 2917 cm^{-1} and 2851 cm^{-1}. Similar characteristic peaks which also result from the C–H stretching and bending were observed in the FTIR spectra of the ZHN–SDS–IC nanocomposite at 2938 cm^{-1}. The peaks that were attributed the asymmetric stretching of S=O appeared in the FTIR spectra for ZHN–SDS–IC at 960 cm^{-1} and ZHN–SDS–IC–CMC at 1203 cm^{-1} [22]. The peaks that were denoted as the absorption peaks for S–O stretching were observed in the FTIR spectra for ZHN–SDS–IC and ZHN–SDS–IC–CMC at 751 cm^{-1} and 820 cm^{-1}, respectively [21]. The absorption peak that indicated the presence of pyridine bonded in the IC structure can be seen in the FTIR spectra for ZHN–SDS–IC at 1609 cm^{-1} and in the FTIR spectra for ZHN–SDS–IC–CMC at 1575 cm^{-1}. This pyridine peak was originally found in the FTIR spectra for the IC at 1559 cm^{-1} [22]. Other characteristic IC peaks that can be observed in the FTIR spectra for ZHN–SDS–IC and ZHN–SDS–IC–CMC are the ones that signify the N–O bond in the nitro group of IC, which appeared at 1431 cm^{-1} and 1479 cm^{-1}, respectively. This peak was also found in the FTIR spectra for IC at 1388 cm^{-1}. The existence of CMC in the ZHN–SDS–IC–CMC nanocomposite was confirmed based on the appearance of the peak that was attributed to the vibration of the symmetrical and asymmetrical stretching of the carboxylate group at 1616 cm^{-1} and 1392 cm^{-1}, respectively [41]. The peak that indicated the –C–O– stretching on the polysaccharide skeleton of the CMC can also be seen in the FTIR spectra for ZHN–SDS–IC–CMC at 1053 cm^{-1}.

The results obtained from the FTIR analysis verified the presence of characteristic peaks for the ZHN–SDS and ZHN–SDS–IC in the ZHN–SDS–CMC and ZHN–SDS–IC–CMC, respectively. The minor displacement of the comparable peaks after the CMC coating process may be observed due to interaction between the CMC and the nanocomposite. The existence of CMC traces was also found in the FTIR spectra for both the ZHN–SDS–CMC and ZHN–SDS–IC–CMC. Therefore, it can be concluded that these results are in good agreement with the PXRD analysis.

Thermal stability studies

The investigation of the thermal stabilities for the ZHN–SDS and ZHN–SDS–IC after undergoing the CMC coating process was performed with TGA/DTG analysis. The TGA/DTG curves for the CMC, ZHN–SDS–CMC and ZHN–SDS–IC–CMC are illustrated in Fig. 5. The thermal decomposition data from the TGA/DTG curves were summarised and matched to the uncoated ZHN–SDS and ZHN–SDS–IC nanocomposite (Table 2). The TGA/DTG analysis revealed that the thermal behaviour for the CMC occurred in two stages. The first one occurred at 82.1 °C with the weight loss of 9.2% due to the evaporation of water and the second stage occurred at 349.5 °C with the weight loss of 66.2% due to the degradation of the CMC [42].

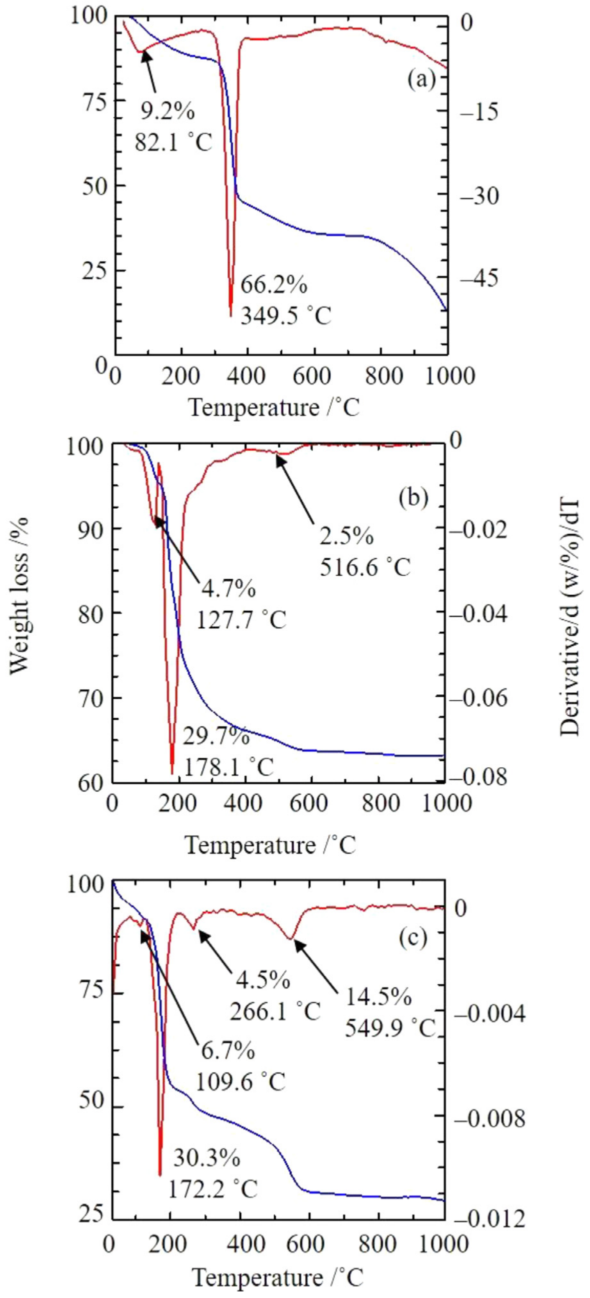

Fig. 5. TGA/DTG curves of (a) CMC, (b) ZHN–SDS–CMC and (c) ZHN–SDS–IC–CMC nanocomposite.

The thermal decomposition of the ZHN–SDS also happened in two stages. A minor weight loss of 3.2% was observed at 107.1 °C and was attributed to the elimination of adsorbed and interlayer water molecules [43]. A greater weight loss occurred at 198.2 °C with 37.2% weight loss that came from the decomposition of SDS. The CMC coating process seemed to cause a slight transformation in the thermal behaviour of the ZHN–SDS because the thermal decomposition of the ZHN–SDS–CMC clearly took place in three stages. Although the first two stages (127.7 °C with 4.7% weight loss and 178.1 °C with 29.7% of weight

Table 2
TGA/DTG data of weight loss for CMC, ZHN–SDS, ZHN–SDS–CMC, ZHN–SDS–IC and ZHN–SDS–IC–CMC.

Thermal decomposition		Samples CMC	ZHN–SDS	ZHN–SDS–CMC	ZHN–SDS–IC	ZHN–SDS IC–CMC
Stage 1	T_{max} (°C)	82.1	107.1	127.7	108.1	109.6
	Percentage (%)	9.2	3.2	4.7	6.2	6.7
Stage 2	T_{max} (°C)	349.5	198.2	178.1	166.4	172.2
	Percentage (%)	66.2	37.2	29.7	31.2	30.3
Stage 3	T_{max} (°C)	–	–	516.6	264.2	266.1
	Percentage (%)	–	–	2.5	3.3	4.5
Stage 4	T_{max} (°C)	–	–	–	595.2	549.9
	Percentage (%)	–	–	–	14.3	14.5
Ref.		Present paper	[35]	Present paper	[35]	Present paper

Abbreviation: CMC, carboxymethyl cellulose; ZHN–SDS, zinc hydroxide nitrate–sodium dodecylsulphate; ZHN–SDS–CMC, zinc hydroxide nitrate–sodium dodecylsulphate–carboxymethyl cellulose; ZHN–SDS–IC, zinc hydroxide nitrate–sodium dodecylsulphate–imidacloprid; ZHN–SDS–IC–CMC, zinc hydroxide nitrate–sodium dodecylsulphate–imidacloprid–carboxymethyl cellulose.

loss) were comparable with the TGA/DTG curve for the ZHN–SDS, an additional thermal decomposition peak was observed at a significantly high temperature (516.6 °C with 2.5% of weight loss). Based on this result, the CMC coating was found to enhance the thermal stability of the ZHN–SDS–CMC.

The thermal decomposition took place in four stages for the ZHN–SDS–IC. The first stage occurred at 108.1 °C (with the weight loss of 6.2%), the second stage at 166.4 °C (with the weight loss of 31.2%) the third stage at 264.2 °C (with the weight loss of 3.3%) and the fourth stage at 595.2 °C (with the weight loss of 14.3%). After the ZHN–SDS–IC was coated with CMC, the thermal decomposition of the ZHN–SDS–IC–CMC also occurred in four stages. The first stage occurred at 109.6 °C (with the weight loss of 6.7%), the second stage at 172.2 °C (with the weight loss of 30.3%), the third stage at 266.1 °C (with the weight loss of 4.5%) and the fourth stage at 549.9 °C (with the weight loss of 14.5%).

Four comparable stages of thermal decomposition possess by ZHN–SDS–IC and ZHN–SDS–IC–CMC indicated that the thermal behaviour of the ZHN–SDS–IC was quite similar after the coating process. The first stage was due to the evaporation of adsorbed water molecules and interlayer water molecules [43]. The second stage came from the decomposition of inorganic moieties of IC and CMC (decomposition of CMC only for ZHN–SDS–IC–CMC). The third stage resulted from the decomposition of the SDS and the fourth stage was due to the collapsing of the layered structure of the nanocomposites [43]. Hence, it can be concluded that even though the CMC coating did not further improve the thermal stabilities of the ZHN–SDS–IC, there was no deterioration of the thermal stability of the ZHN–SDS–IC–CMC either. The temperature of the final thermal decomposition that happened above 500 °C is reasonably high, therefore the ZHN–SDS–IC–CMC still had good thermal stability after the coating process.

Surface morphology analysis

Fig. 6 shows the FESEM micrographs of the CMC, ZHN–SDS, ZHN–SDS–CMC, ZHN–SDS–IC and ZHN–SDS–IC–CMC nanocomposites. The CMC morphology is observed to be smooth and even, which is in good agreement with recent literature [27]. The ZHN–SDS can be described as having a tabular, stacked plate-like structure and sharp edges, which is the expected morphology for a layered material, as reported elsewhere. The presence of the CMC coatings began to smoothen the surface of the ZHN–SDS–CMC and caused the surface to become more compact and uneven. The FESEM micrograph of ZHN–SDS–CMC shows a great resemblance to the surface morphology of the CMC, although stacked plate-like structure for the ZHN–SDS can still be vaguely observed.

The ZHN–SDS–IC nanocomposites had an agglomerated, thin plate-like structure with more rounded edges. As observed from the FESEM micrograph for the ZHN–SDS–IC–CMC, some noticeable modification can be seen after the CMC coating process. Similar to the ZHN–SDS–CMC, the CMC coating causing the surface of the ZHN–SDS–IC–CMC to be covered by the CMC layer, hence making the surface flatter and more compact. The addition of CMC softened the texture of the ZHN–SDS–IC, resulting to an overall relaxation, and made the former plate-like features of the ZHN–SDS–IC to appear less obvious. The results obtained from the surface morphology analysis by FESEM showed that the CMC coating process brought about some morphological transformation for the surface texture of both the ZHN–SDS–CMC and ZHN–SDS–IC–CMC nanocomposites, while they vaguely maintained their original features.

Release study of ZHN–SDS–IC–CMC nanocomposite into aqueous solutions of binary and ternary phosphate, sulphate and chloride systems

This present section will be focussed on investigating the influence of the type of release media and their concentration on the release behaviour of the IC from the interlayer gallery of the ZHN–SDS–IC–CMC. The characterization of the release behaviour will be made based on the observation on the maximum percentage released and the time taken for the release process. The release behaviour of the IC from the ZHN–SDS–IC–CMC nanocomposite obtained in this study will be compared to the results in the authors' previously published paper that reported on the release of IC from ZHN–SDS–IC. The role of CMC in the release process will be thoroughly discussed as well.

The release study of the ZHN–SDS–IC–CMC nanocomposite was performed in release media containing PO_4^{3-}, SO_4^{2-} and Cl^-. This was done because IC is a type of insecticide that is typically used in paddy cultivation areas and these are the types of anions that would be commonly available in those areas. For the release study of IC from ZHN–SDS–IC–CMC in single system, the aqueous solutions of Na_3PO_4, Na_2SO_4 and NaCl were prepared in three different concentrations, namely 0.1 M, 0.3 M and 0.5 M. As for the release study of IC from ZHN–SDS–IC–CMC in binary and ternary system of aqueous solutions, the aqueous solutions with the combination of PO_4^{3-}–SO_4^{2-}, PO_4^{3-}–Cl^-, SO_4^{2-}–Cl^- and PO_4^{3-}–SO_4^{2-}–Cl^- were used as release medium. The release profiles for the IC from the ZHN–SDS–IC–CMC nanocomposite into the aqueous solution are shown in Fig. 7.

The tendency of intercalated IC to be released from the interlayer gallery of the ZHN–SDS nanocomposite comes from the ion exchange ability of ZHN–SDS. The higher charge density for the PO_4^{3-} compared to the other anions increased the possibility for the PO_4^{3-} to be attracted to the positively charged ZHN–SDS layer so as to be exchanged with the

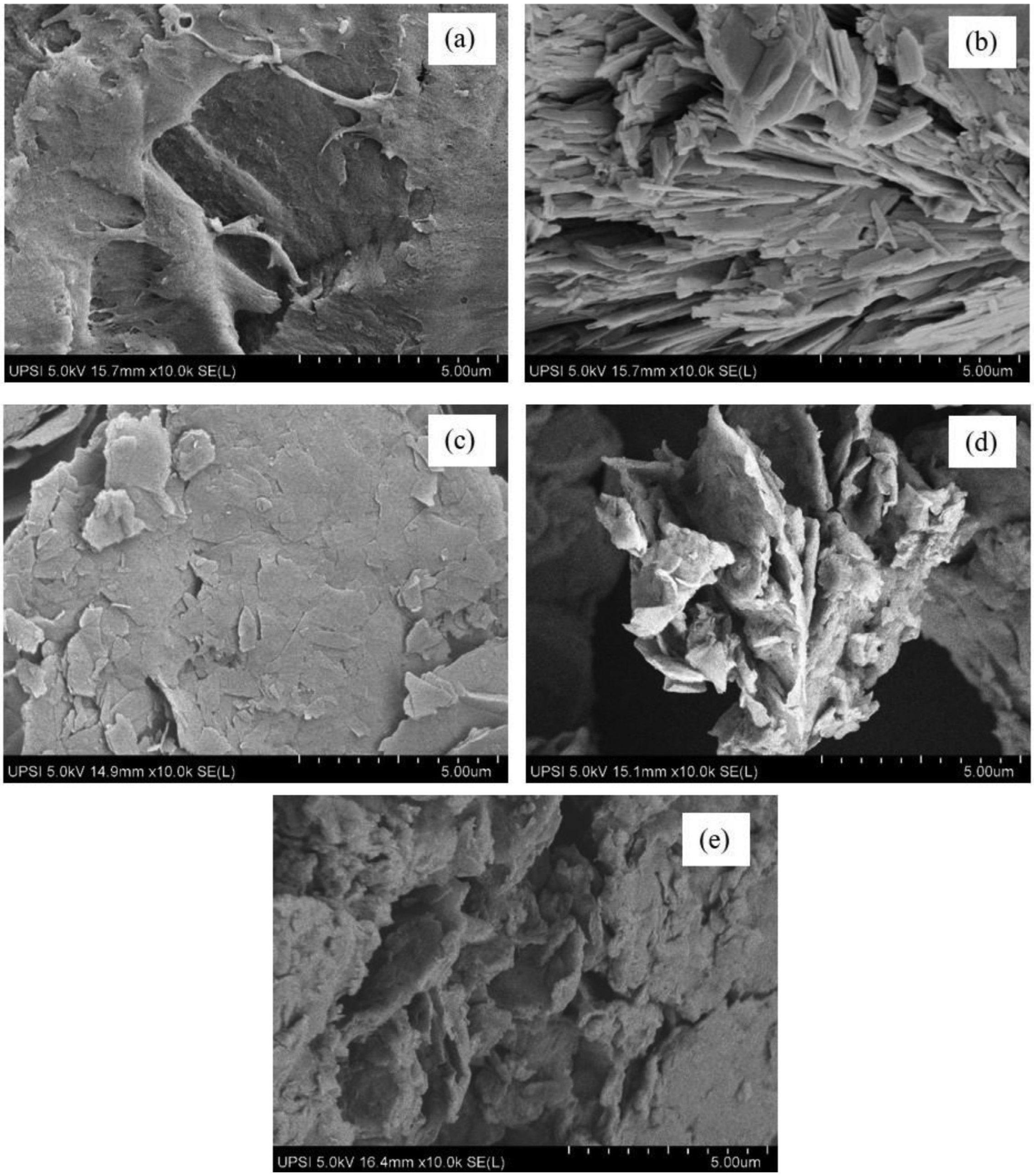

Fig. 6. Surface morphology of (a) carboxymethyl cellulose, (b) ZHN–SDS, (c) ZHN–SDS–CMC, (d) ZHN–SDS–IC and (e) ZHN–SDS–IC–CMC.

intercalated IC. This release behaviour is consistent with what was already observed because the release profiles revealed the highest release occurred when the release process was carried out in aqueous solution of Na_3PO_4 (96.8 %), followed by the release in Na_2SO_4 (95.8 %) and NaCl (94.9 %). A higher maximum percentage of released IC occurred when the ZHN–SDS–IC–CMC nanocomposites were exposed to release media that contained anions with a higher charge density. This indicated that the release behaviour of the IC was greatly affected by the type of ions present in the release media.

The release profile also demonstrated that varying the concentration of the release media had a considerable influence on the maximum percentage of released IC as well. The maximum percentages of released IC in an aqueous solution of Na_3PO_4 were found to be 83.3% (0.1 M), 93.2% (0.3 M) and 96.8% (0.5 M). In the aqueous solution of Na_2SO_4, the maximum percentages of released IC were 68.2% (0.1 M), 92.6% (0.3 M), and 95.8% (0.5 M). In the aqueous solution of NaCl, the maximum percentages of release IC were 57.6% (0.1 M), 91.6% (0.3 M) and 94.9% (0.5 M). The overall release process was found to exhibit a similar release trend when the release was performed in different concentrations of the release media. The maximum percentage of released IC was observed to increase when the ZHN–SDS–IC–CMC was immersed in a higher concentration of the release media. The higher amounts of anions that were provided in a higher concentration of release media assisted the ion exchange process between the release media and the IC and increased the maximum percentage release.

Instead of comparing the release behaviour according to their maximum released percentage, the release behaviour can also be characterized based on the time taken by the ZHN–SDS–IC–CMC nanocomposite to release the IC up to its maximum value. The release study that was performed in an aqueous solution of NaCl seemed to take the longest time to reach its maximum release percentage. The time required for the release process in 0.1 M, 0.3 M and 0.5 of NaCl was 3023 min, 1670 min

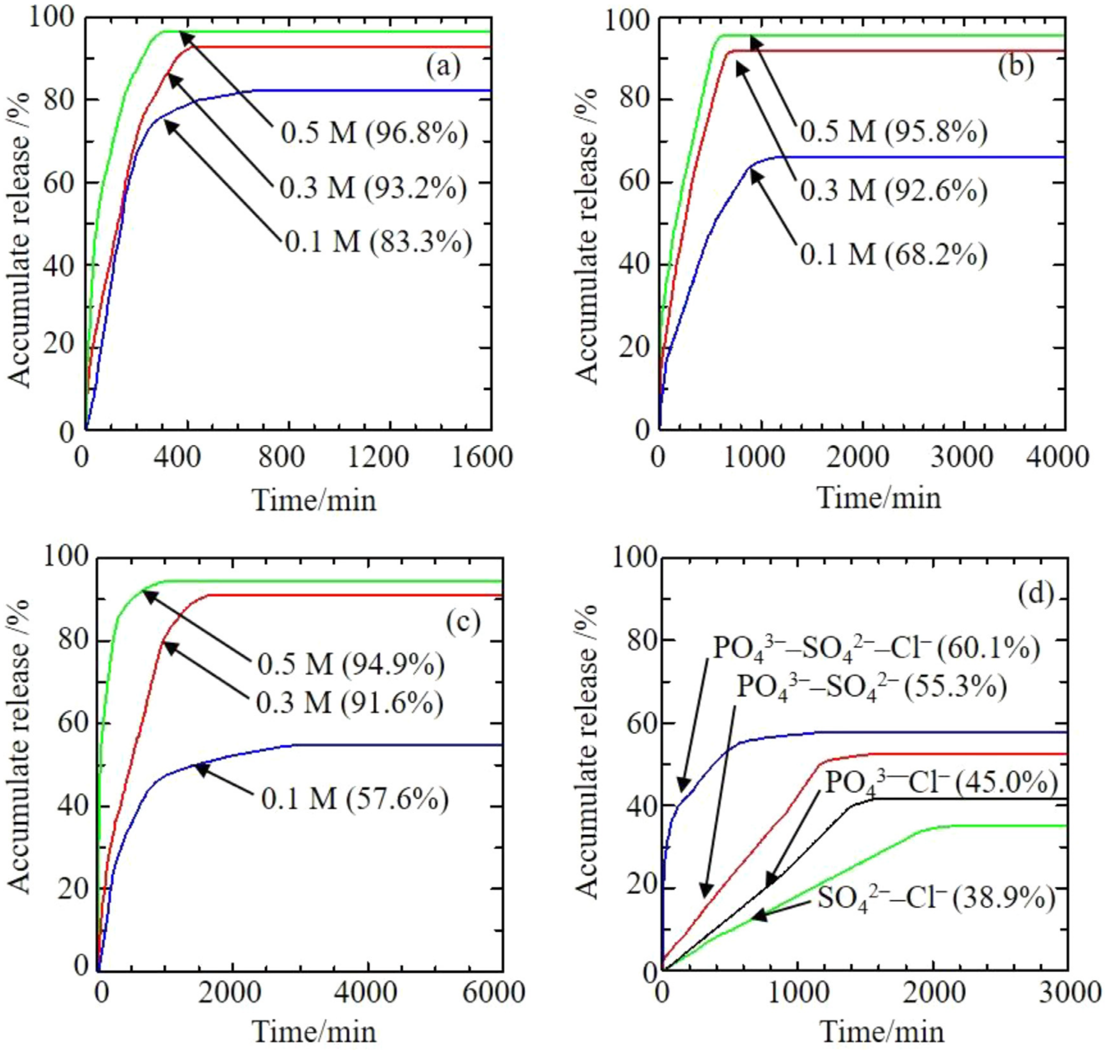

Fig. 7. Release profiles of IC from ZHN–SDS–IC–CMC nanocomposite into (a) sodium phosphate, (b) Sodium sulphate, (c) sodium chloride and (d) phosphate, sulphate and chloride mixture.

Table 3
The comparison of the percentage release from ZHN–SDS–IC and ZHN–SDS–IC–CMC into various aqueous solutions.

Aqueous solutions			ZHN–SDS–IC Percentage release (%)	Release time (min)	ZHN–SDS–IC–CMC Percentage release (%)	Release time (min)
Single	PO_4^{3-}	0.1 M	28.6	310	83.3	675
		0.3 M	74.0	173	93.2	420
		0.5 M	91.0	83	96.8	310
	SO_4^{2-}	0.1 M	15.7	689	68.2	1292
		0.3 M	82.3	473	92.6	726
		0.5 M	85.5	302	95.8	631
	Cl^-	0.1 M	6.2	1478	57.6	3023
		0.3 M	83.9	793	91.6	1670
		0.5 M	84.9	549	94.9	1028
Binary	PO_4^{3-}–SO_4^{2}		82.3	1320	55.3	1640
	PO_4^{3-}–Cl^-		24.4	1378	45.0	1666
	SO_4^{2}–Cl^-		22.0	1426	38.9	2228
Ternary	PO_4^{3-}–SO_4^{2}–Cl^-		83.9	716	60.1	1151
Ref.			[35]		Present paper	

Abbreviation: ZHN–SDS–IC, zinc hydroxide nitrate–sodium dodecylsulphate–imidacloprid; ZHN–SDS–IC–CMC, zinc hydroxide nitrate–sodium dodecylsulphate–imidacloprid–carboxymethyl cellulose.

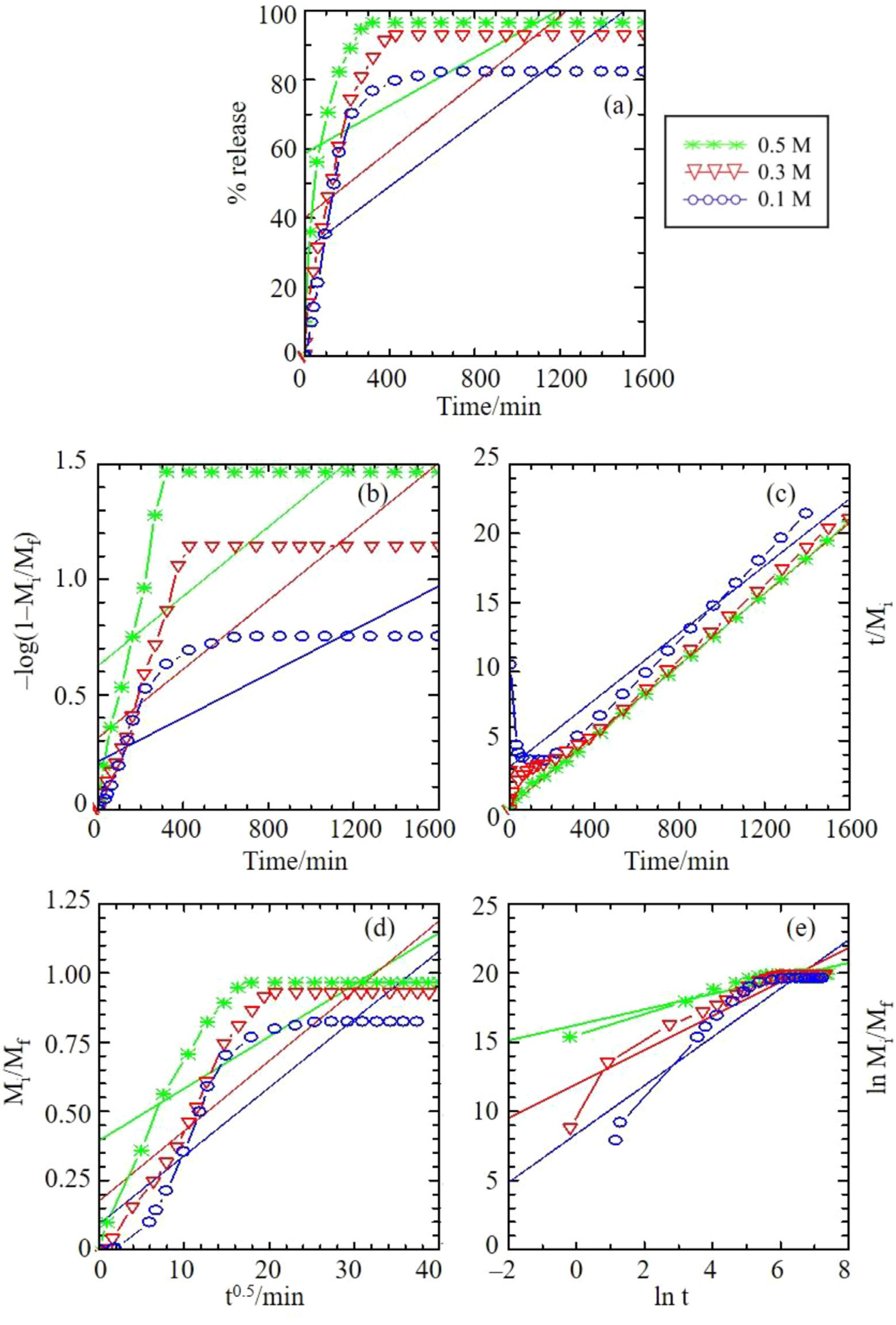

Fig. 8. Fitting of the data for IC release from ZHN–SDS–IC–CMC nanocomposite into sodium phosphate solution for the (a) zeroth-order, (b) first-order, (c) pseudo-second-order, (d) parabolic diffusion and (e) Fickian diffusion models.

and 1028 min, respectively. Owing to the monovalent nature of Cl^-, the Cl^- has a lower affinity compared to the PO_4^{3-} and SO_4^{2-} and a slower exchange process between the IC and the Cl^- [44–46]. As for the release study that was performed in an aqueous solution of Na_2SO_4, the times taken by the ZHN–SDS–IC–CMC nanocomposite to reach its maximum release were 1292 min (0.1 M), 726 min (0.3 M) and 631 min (0.5 M). When aqueous solution of Na_3PO_4 was used as release media, the times it took for the release process were 675 min (0.1 M), 420 min (0.3 M), and 310 min (0.5 M). Hence, the time for the release decreased in the order of NaCl > Na_2SO_4 > Na_3PO_4. The release study that was conducted in a lower concentration of release media also demonstrated a slower release rate compared to the release in a higher concentration of release media due to the lesser number of anions available [45].

For the release study of ZHN–SDS–IC–CMC in binary aqueous solutions, the aqueous solutions with the combination of PO_4^{3-}–SO_4^{2-}, PO_4^{3-}–Cl^- and SO_4^{2-}–Cl^- were used as release medium, whereas a aqueous solution with the combination of PO_4^{3-}–SO_4^{2-}–Cl^- was used as the release medium for the release study in the ternary system. Based on the release profile obtained, it was observed that the release of IC from the ZHN–SDS–IC–CMC nanocomposite was significantly affected by the type of anions provided by the release medium. Different combinations

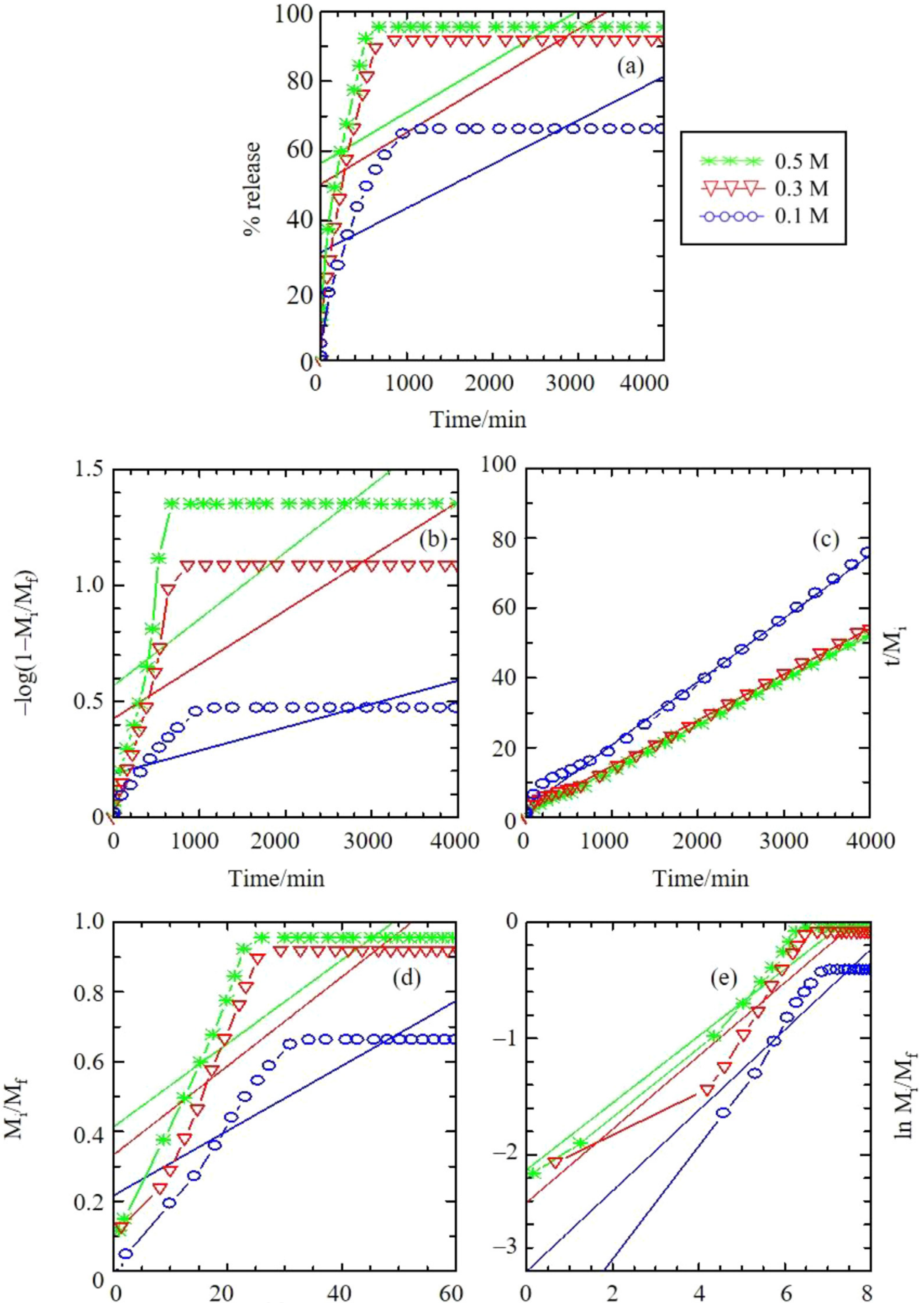

Fig. 9. Fitting of the data for IC release from ZHN–SDS–IC–CMC nanocomposite into sodium sulphate solution for the (a) zeroth-order, (b) first-order, (c) pseudo-second-order, (d) parabolic diffusion and (e) Fickian diffusion models.

of anions in the release medium brought into certain changes on the release behaviour of IC, specifically in term of the percentage of their accumulated release and the duration for the release process. The highest percentage of the accumulated release was recoded when the release of IC was conducted in the ternary system of aqueous solution, which contain all three anions. In the ternary system release medium, 60.1% of IC was released to the interlayer gallery of the ZHN–SDS–IC–CMC nanocomposite within 1151 min, thus demonstrating that the release in this release medium happened in the fastest release rate of all release medium containing multiple anions. The second highest percentage of accumulated release was obtained when the release is conducted in the aqueous solution of PO_4^{3-}–SO_4^{2-}, which releasing 55.3% of the intercalated IC in 1640 min, followed by the release in the aqueous solution of PO_4^{3-}–Cl^-, which involved the release of 45.0% of intercalated IC within 1666 min. The slowest release process with the lowest percentage of accumulated release was observed when the aqueous solution of SO_4^{2-}–Cl^- was used as release medium, which requires up to 2228 min in order to reach 38.9% release.

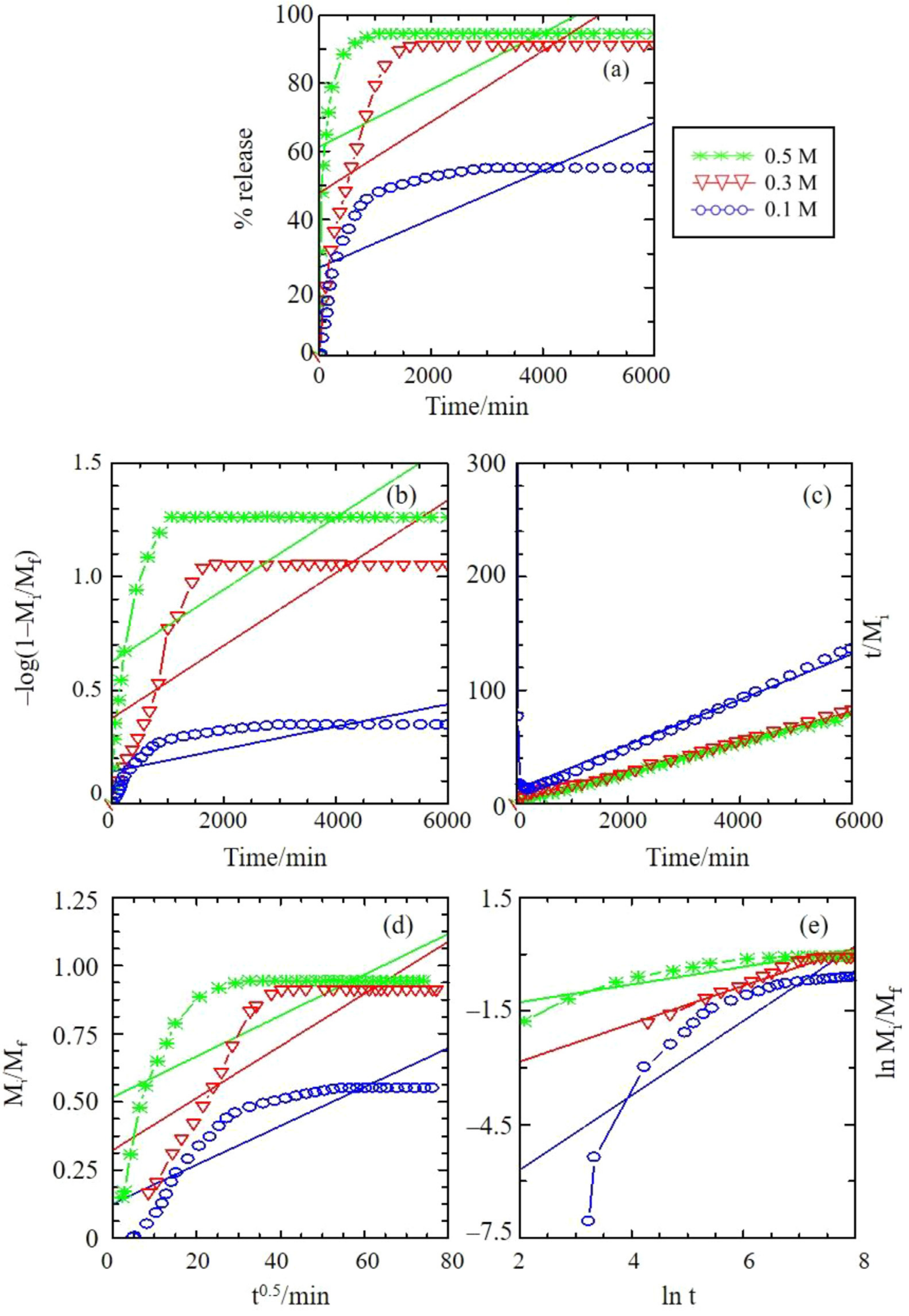

Fig. 10. Fitting of the data for IC release from ZHN–SDS–IC–CMC nanocomposite into sodium chloride solution for the (a) zeroth-order, (b) first-order, (c) pseudo-second-order, (d) parabolic diffusion and (e) Fickian diffusion models.

Based on the release profile, it can be seen that the release of IC in binary and ternary systems demonstrates a noticeable pattern. Whenever the PO_4^{3-} anion was used as one of the components in the release medium, the release process was found to occur at a higher release rate and reach a higher percentage release of IC. The domination of the PO_4^{3-} anion on the whole release process is contributed to by the fact that the PO_4^{3-} anion is a trivalent anion, which possesses better affinity toward the positively charged host layer, as compared to SO_4^{2-} and Cl^- [46]. On the basis of a similar fact, the presence of the Cl^- anion demonstrates a slower release process with a lower percentage release. The release behaviour of the IC from the ZHN–SDS–IC–CMC nanocomposite was then compared with the result obtained in a previous study that elucidate the release behaviour of IC from the ZHN–SDS–IC nanocomposite, which is summarised in Table 3. This comparison was made so that the impact of the CMC coating on the release behaviour can be observed.

Based on the comparison made in Table 3, the time taken by the ZHN–SDS–IC–CMC nanocomposite to reach its maximum IC release was

Table 4
Comparison of rate constants, *k*, and regression values, r^2, obtained from the fitting of the data of release from ZHN–SDS–IC–CMC into aqueous solution of Na_3PO_4, Na_2SO_4 and NaCl.

Aqueous solution		Zeroth-order r^2	First-order r^2	Parabolic diffusion r^2	Fickian diffusion r^2	Pseudo-second-order r^2	K ($\times 10^{-3}$ s^{-1})	$t_{1/2}$
Na_3PO_4	0.1 M	0.589	0.681	0.823	0.867	0.886	0.109	115
	0.3 M	0.552	0.675	0.801	0.872	0.999	0.112	112
	0.5 M	0.392	0.553	0.639	0.876	0.999	0.315	40
Na_2SO_4	0.1 M	0.542	0.606	0.747	0.862	0.996	0.041	305
	0.3 M	0.481	0.588	0.716	0.908	0.998	0.062	203
	0.5 M	0.416	0.545	0.665	0.948	0.999	0.080	157
NaCl	0.1 M	0.565	0.627	0.776	0.749	0.916	0.033	385
	0.3 M	0.543	0.640	0.720	0.960	0.996	0.035	363
	0.5 M	0.379	0.505	0.592	0.836	1.00	0.360	35

generally twice much compared to the time required by the ZHN–SDS–IC nanocomposite. The significant time delay shows that the CMC coating did contribute to prolonging the release of the IC from the interlayer gallery of the ZHN–SDS–IC–CMC. The potential of the CMC to slow the release of the IC is due to the characteristics of the CMC itself, such as being strongly hygroscopic and hydrophilic nature and having an adequate swelling characteristic and gelation ability [47,48]. Due to these properties, it is possible for the CMC to develop an external gel layer on the outer surface of the ZHN–SDS–IC–CMC nanocomposite, which acted as an additional barrier in slowing the release of the intercalated IC. The gel layer was formed when the ZHN–SDS–IC–CMC was exposed to the aqueous solution and generated the formation of a steep water concentration gradient between the aqueous solution and the CMC coating that was present on the outermost surface of the ZHN–SDS–IC–CMC nanocomposite. This triggered the water imbibition into the CMC and lead to the formation of the gel layer.

The overall release process of intercalated ions from a strongly hydrophilic matrix, like CMC, commonly results from the water diffusion into the CMC matrix, the swelling of CMC and the diffusion of the intercalated ions from the swollen CMC into the release media [49]. However, in order to obtain further information regarding the mechanism of the release process, the release data were fitted into several kinetic models, which will be discussed in the subsequent section.

Kinetic study of IC from the ZHN–SDS–IC–CMC nanocomposite into various aqueous solution

The kinetic study of the IC from the ZHN–SDS–IC–CMC nanocomposite was conducted by fitting the kinetic data obtained from the release study into zeroth-order (Eq. (i)) [50], first-order (Eq. (ii)) [51], pseudo-second order (Eq. (iii)) [52], parabolic diffusion (Eq. (iv)) [53] and Fickian diffusion (Eq. (v)) model kinetics. Fitting of the data for the IC release from the ZHN–SDS–IC–CMC nanocomposite into aqueous solutions of Na_3PO_4, Na_2SO_4 and NaCl are illustrated in Figs. 8, 9 and 10, respectively. The equation for each release kinetic models that was used for each type of fitting is:

$$x = t + c \tag{1}$$

$$-\log\left(1 - -M_i/M_f\right) = t + c \tag{2}$$

$$t/M_i = 1/{M_f}^2 + t/M_f \tag{3}$$

$$M_i/M_f = kt^{0.5} + c \tag{4}$$

$$M_i/M_f = kt^n \tag{5}$$

where *x* refers to percentage release of IC from the interlayer gallery of ZHN–SDS–IC–CMC at time, *t*; *c* represents a constant; and M_i and M_f, are the initial and final concentrations of the IC, respectively. The value of the rate constant, *k*, regression values, r^2, and diffusion exponent value, *n*, were calculated from the above equations. The half time, $t_{1/2}$, which represents the time required by the ZHN–SDS–IC–CMC to release the IC until half of its maximum percentage is released, was obtained from the release profile. The comparison of $t_{1/2}$, *k* and r^2 for the release process in the release media of Na_3PO_4, Na_2SO_4 and NaCl are summarised in Table 4. The fitting with the r^2 value that is the closest to 1 was chosen as the best fit for the release data.

The fitting of the data and the summary in Table 4 revealed that the release of the IC from the ZHN–SDS–IC–CMC nanocomposite in aqueous solutions of Na_3PO_4, Na_2SO_4 and NaCl as the release media was best described using a pseudo-second order kinetic model. The linearization of the release into the pseudo-second order kinetic model suggested that this kinetic model is the best fit for the release data, with the r^2 value obtained in the range of $0.886 > r^2 > 1.00$. This result indicates that the mechanism involved in releasing the intercalated IC was through a dissolution and ion exchange process.

These mechanisms can be explained based on the hygroscopic nature and gelation forming ability of the CMC. As previously mentioned in the kinetic study section, the water diffusion into the CMC matrix caused the swelling of the CMC, which then triggered the formation of a thick, gelatinous and viscous gel layer that encapsulated the outer surface of the ZHN–SDS–IC–CMC. The constant exposure of the ZHN–SDS–IC–CMC in an aqueous environment during the release process resulted in a continuous inward ingression of water into the swollen CMC gel layer. This consequently initiated the disentanglement of the CMC polymeric chain and gradual dissolution of the CMC gel layer, which allowed the slow release of the intercalated SDS and IC into the release media. The release of the intercalated SDS and IC caused the overall charge of the ZHN–SDS–IC–CMC nanocomposite to be unbalanced. The anions provided in the release media were then naturally attracted into the excessively positively charged ZHN layer and entered the interlayer gallery via the ion exchange process so that the unbalanced charge could be counterbalanced. The impact of hygroscopic nature and gelation forming ability of CMC in slowing the release of IC as agrees well with recent studies [47,54].

The $t_{1/2}$ values were found to be the highest, with the value of 385 when the aqueous solution of NaCl was used as the release media for the IC, hence proving that the release process was the slowest in this release media. The $t_{1/2}$ values were found to be the second highest when the release was performed in aqueous solution of Na_2SO_4 and third highest with Na_3PO_4. These findings revealed that the charge density of the anions provided by the release media played a significant role in controlling the release rate of the intercalated IC. A clear increase in the $t_{1/2}$ values can also be seen when the lower concentration of the release media were used in the release process due to the fact that release media of lower concentration provided fewer anions compared to the release media of a higher concentration. The lower concentration led to slower release process [55].

Conclusion

The physicochemical characterization performed with PXRD and FTIR revealed that the additional CMC did not cause any alteration in the type if ions intercalated in the interlayer gallery of ZHN–SDS–IC–CMC. It was also observed that the CMC was only adsorbed on the surface therefore the success of the CMC coating process was verified. Although the result obtained from the TGA/DTG did not show any enhancement on the thermal stability of ZHN–SDS–IC–CMC, the temperature of the final thermal decomposition (above 500 °C) was considerably high and proved that the ZHN–SDS–IC–CMC still preserved a good thermal stability after the coating process. The morphology analysis showed that the addition of the CMC softened the texture of the ZHN–SDS–IC and made the surface flatter and more compact while the original features were vaguely maintained. The release study performed using UV/Vis spectrometry showed that when the ZHN–SDS–IC was coated with CMC, a noticeable increase in the time taken by the ZHN–SDS–IC–CMC nanocomposite to reach the maximum IC release was observed and proved the potential to prolong the release of the IC. The fitting of the release data into several kinetic models revealed that the release of the IC from the ZHN–SDS–IC–CMC in all release media was best described with a pseudo-second order kinetic model. This indicated that the mechanisms involved in releasing the intercalated IC went through a dissolution and ion exchange process. The findings of this study showed that the CMC coating has a great potential to improve the CRF properties of ZHN–SDS–IC nanocomposite. Hence, the ZHN–SDS–IC–CMC can be used to manufacture a greener and safer insecticide that will benefit communities and the environment.

Declaration of Competing Interest

The authors declare that they have no known competing financial interests or personal relationships that could have appeared to influence the work reported in this paper.

CRediT authorship contribution statement

Sharifah Norain Mohd Sharif: Conceptualization, Methodology, Data curtion, Writing – original draft. **Norhayati Hashim:** Supervision, Funding acquisition, Writing – review & editing. **Illyas Md Isa:** Supervision, Conceptualization, Methodology. **Suriani Abu Bakar:** Conceptualization, Data curtion. **Mohamad Idris Saidin:** Methodology, Writing – review & editing. **Mohamad Syahrizal Ahmad:** Conceptualization, Writing – review & editing. **Mazidah Mamat:** Data curtion, Writing – review & editing. **Mohd Zobir Hussein:** Writing – review & editing, Project administration. **Rahadian Zainul:** Conceptualization, Methodology. **Azlan Kamari:** Methodology, Writing – review & editing.

Acknowledgement

The authors wish to thank UPSI and Ministry of Education Malaysia for the support during completing the research.

Author contributions

The manuscript was written through contributions of all authors. All authors have given approval to the final version of the manuscript.

Funding sources

This work was supported by the GPU-RISING STAR Grant No. 2019-0119-103-01.

Notes

The authors declare no competing interests.

Research data

Due to confidentiality issues, the raw data of the study would remain confidential and would not be shared.

Supplementary materials

Supplementary material associated with this article can be found, in the online version, at doi:10.1016/j.chphi.2021.100017.

References

[1] E. Gonzalez-Pradas, M. Fernandez-Perez, M. Villafranca-Sanchez, F. Martinez-Lopez, F. Flores-Cespedes, Use of bentonite and humic acid as modifying agents in alginate-based controlled-release formulations of imidacloprid, Pestic. Sci. 55 (1999) 546–552.

[2] I. Ishaaya, A.R. Horowitz, in: Insecticides with Novel Modes of Action, Springer, Berlin, Heidelberg, 1998, pp. 1–24.

[3] W. Yuan, Q. Solihin, Zhang, J. Kano, F. Saito, Mechanochemical formation of K-Si–Ca-O compound as a slow-release fertilizer, Powder Technol. 260 (2014) 22–26.

[4] C.A. Bernal Rodriguez, V.L. Bassani, L. Castellanos, F.A. Ramos Rodríguez, Y. Baena, Development of an oral control release system from Physalis peruviana L. fruits extract based on the co-spray-drying method, Powder Technol. 354 (2019) 676–688.

[5] S.N.M. Sharif, N. Hashim, I.M. Isa, S.A. Bakar, M.I. Saidin, M.S. Ahmad, M. Mamat, M.Z. Hussein, Controlled release formulation of zinc hydroxide nitrate intercalated with sodium dodecylsulphate and bispyribac anions: a novel herbicide nanocomposite for paddy cultivation, Arab. J. Chem. 13 (2019) 4513–4527.

[6] R. Grillo, A.E.S.S. Pereira, C.S. Nishisaka, R. De Lima, K. Oehlke, R. Greiner, L.F. Fraceto, Chitosan/tripolyphosphate nanoparticles loaded with paraquat herbicide: an environmentally safer alternative for weed control, J. Hazard. Mater. 278 (2014) 163–171.

[7] J.L. De Oliveira, E.V.R. Campos, M. Bakshi, P.C. Abhilash, L.F. Fraceto, Application of nanotechnology for the encapsulation of botanical insecticides for sustainable agriculture: prospects and promises, Biotechnol. Adv. 32 (2014) 1550–1561.

[8] M.Z. Hussein, N.F. Nazarudin, S.H. Sarijo, M.A. Yarmo, Synthesis of a layered organic-inorganic nanohybrid of 4-chlorophenoxyacetate-zinc-layered hydroxide with sustained release properties, J. Nanomater. 2012 (2012) 1–10.

[9] S. Dubey, V. Jhelum, P.K. Patanjali, Controlled release agrochemicals formulations: a review, J. Sci. Ind. Res. 70 (2011) 105–112.

[10] N. Hashim, M.Z. Hussein, I. Isa, A. Kamari, A. Mohamed, A.M. Jaafar, H. Taha, Synthesis and controlled release of cloprop herbicides from cloprop-layered double hydroxide and cloprop-zinc-layered hydroxide nanocomposites, Open J. Inorg. Chem. 4 (2014) 1–9.

[11] A.M. Bashi, Synthesis of nano particle ZnO-organic nanohybrid and its role in controlled release of 4-chlorophenoxy acetate from the lamella of ZnO nanocomposite, J. Kerbala Univ. 7 (2009) 1–8.

[12] I.M. Isa, S.N.M. Sharif, N. Hashim, S.A. Ghani, Amperometric determination of nanomolar mercury(II) by layered double nanocomposite of zinc/aluminium hydroxide-3(4-methoxyphenyl)propionate modified single-walled carbon nanotube paste electrode, Ionics 21 (2015) 2949–2958.

[13] I.M. Isa, S.N.A. Dahlan, N. Hashim, M. Ahmad, S.A. Ghani, Electrochemicals sensor for cobalt(II) by modified carbon paste electrode with Zn/Al-2(3-chlorophenoxy)propionate nanocomposite, Int. J. Electrochem. Sci. 7 (2012) 7797–7808.

[14] N.I. Wardani, I.M. Isa, N. Hashim, S.A. Ghani, Zinc layered hydroxide-2(3-chlorophenoxy)propionate modified multi-walled carbon nanotubes paste electrode for the determination of nano-molar levels copper(II), Sens. Actuat. B Chem. 198 (2014) 243–248.

[15] R. Zainul, N.A. Azis, I.M. Isa, N. Hashim, M.S. Ahmad, M.I. Saidin, S. Mukdasai, Zinc/aluminium–quinclorac layered nanocomposite modified multi-walled carbon nanotube paste electrode for electrochemical determination of bisphenol A, Sensors 19 (2019) 941.

[16] I.N.F.A. Aziz, S.H. Sarijo, F.S.M. Rajidi, R. Yahaya, M. Musa, Synthesis and characterization of novel 4-aminobenzoate interleaved with zinc layered hydroxide for potential sunscreen application, J. Porous Mater. 26 (2019) 717–722.

[17] M.S. Ahmad, I.M. Isa, N. Hashim, S.M. Si, M.I. Saidin, A highly sensitive sensor of paracetamol based on zinc-layered hydroxide-L-phenylalanate-modified multi-walled carbon nanotube paste electrode, J. Solid State Electrochem. 22 (2018) 2691–2701.

[18] N. Hashim, Z. Muda, S.A. Hamid, I. Isa, A. Kamari, A. Mohamed, Z. Hussein, S.A. Ghani, Characterization and controlled release formulation of agrochemical herbicides based on zinc-layered hydroxide-3-(4-methoxyphenyl)propionate nanocomposite, J. Phys. Chem. Sci. 1 (2014) 1–6.

[19] G.S. Mac Hado, G.G.C. Arízaga, F. Wypych, S. Nakagaki, Immobilization of anionic metalloporphyrins on zinc hydroxide nitrate and study of an unusual catalytic activity, J. Catal. 274 (2010) 130–141.

[20] G.G.C. Arizaga, A.S. Mangrich, J.E.F. da Costa Gardolinski, F. Wypych, Chemical modification of zinc hydroxide nitrate and Zn-Al-layered double hydroxide with dicarboxylic acids, J. Colloid Interface Sci. 320 (2008) 168–176.

[21] J. Liu, X. Zhang, Y. Zhang, Preparation and release behavior of chlorpyrifos adsolubilized into Layered zinc hydroxide nitrate intercalated with dodecylbenzenesulfonate, ACS Appl. Mater. Interfaces 7 (2015) 11180–11188.

[22] D.P. Qiu, W.G. Hou, J. Xu, J. Liu, S. Liu, Synthesis and characterization of imidacloprid/hydrotalcite-like compound nanohybrids, Chin. J. Chem. 27 (2009) 1879–1885.

[23] A.K. Srivastava, Advances in Citrus Nutrition editor, Springer Science & Business Media, New York, 2012.

[24] Li, J., Li, Y., Dong, H., Controlled release of herbicide acetochlor from clay/carboxylmethylcellulose gel formulations. *J. Agric. Food Chem.*56 (2008) 1336–1342.

[25] Corradini, E., De Moura, M.R., Mattoso, L.H.C., A preliminary study of the incorparation of NPK fertilizer into chitosan nanoparticles. *Exp. Polym. Lett.*4 (2010) 509–515.

[26] Luo, Y., Teng, Z., Li, Y., Wang, Q., Solid lipid nanoparticles for oral drug delivery: chitosan coating improves stability, controlled delivery, mucoadhesion and cellular uptake. *Carbohydr. Polym.*122 (2015) 221–229.

[27] Akalin, G.O., Pulat, M., Preparation and Characterization of Nanoporous Sodium Carboxymethyl Cellulose Hydrogel Beads 2018 (2018).

[28] Akalin, G.O., Pulat, M., Controlled release behavior of zinc-loaded carboxymethyl cellulose and carrageenan hydrogels and their effects on wheatgrass growth. *J. Polym. Res.*27 (2020).

[29] Pulat, M., Tan, N., Onurdag, F.K., Swelling dynamics of IPN hydrogels including acrylamide-acrylic acid-chitosan and evaluation of their potential for controlled release of piperacillin-tazobactam. *J. Appl. Polym. Sci.*116 (2010) 2658–2667.

[30] Pulat, M., Özgündüz, H.I., Swelling behavior and morphological properties of semi-IPN hydrogels based on ionic and non-ionic components. *Biomed. Mater. Eng.*24 (2014) 1725–1733.

[31] Pulat, M., Uğurlu, N., Preparation and characterization of biodegradable gelatin-PAAm-based IPN hydrogels for controlled release of maleic acid to improve the solubility of phosphate fertilizers. *Soft Mater.*14 (2016) 217–227.

[32] Akalin, G.O., Pulat, M., Preparation and characterization of κ-carrageenan hydrogel for controlled release of copper and manganese micronutrients. *Polym. Bull.*77 (2020) 1359–1375.

[33] Pulat, M., Department, D.A., Fluconazole release through semi-interpenetrating polymer network hydrogels based on chitosan, acrylic acid, and citraconic acid. *J. Appl. Polym. Sci.*113 (2009) 2613–2619.

[34] Pulat, M., Eksi, H., Determination of swelling behavior and morphological properties of poly(acrylamide-co-itaconic acid) and poly(acrylic acid-co-itaconic acid) copolymeric hydrogels. *J. Appl. Polym. Sci.*102 (2006) 5994–5999.

[35] Sharif, S.N.M., Hashim, N., Isa, I.M., Bakar, S.A., Saidin, M.I., Ahmad, M.S., Mamat, M., Hussein, M.Z., Surfactant-assisted imidacloprid intercalation of layered zinc hydroxide nitrate: synthesis, characterisation and controlled release formulation. *J. Porous Mater.*27 (2020) 473–486.

[36] Kura, A.U., Hussein-Al-Ali, S.H., Hussein, M.Z., Fakurazi, S., Preparation of Tween 80-Zn/Al-levodopa-layered double hydroxides nanocomposite for drug delivery system. *Sci. World J.* (2014) doi:10.1155/2014/104246.

[37] Sanjai, C., Kothan, S., Gonil, P., Saesoo, S., Sajomsang, W., Chitosan-triphosphate nanoparticles for encapsulation of super-paramagnetic iron oxide as an MRI contrast agent. *Carbohydr. Polym.*104 (2014) 231–237.

[38] Hussein, M.Z., Rahman, N.S.S.A., Sarijo, S.H., Zainal, Z., Synthesis of a dual herbicides- intercalated layered zinc hydroxide nanohybrid with simultaneous controlled release property of the two herbicides. *Int. J. Mol. Sci.*13 (2011) 7328–7342.

[39] Li, M., Chen, S., Ni, F., Wang, Y., Wang, L., Layered double hydroxides functionalized with anionic surfactant: direct electrochemistry and electrocatalysis of hemoglobin. *Electrochim. Acta*53 (2008) 7255–7260.

[40] Tao, Q., Yuan, J., Frost, R.L., He, H., Yuan, P., Zhu, J., Effect of surfactant concentration on the stacking modes of organo-silylated layered double hydroxides. *Appl. Clay Sci.*45 (2009) 262–269.

[41] Yadollahi, M., Namazi, H., Barkhordari, S., Preparation and properties of carboxymethyl cellulose/layered double hydroxide bionanocomposite film. *Carbohydr. Polym.*108 (2014) 83–90.

[42] Angadi, S.C., Manjeshwar, L.S., Aminabhavi, T.M., Interpenetrating polymer network blend microspheres of chitosan and hydroxyethyl cellulose for controlled release of isoniazid. *Int. J. Biol. Macromol.*47 (2010) 171–179.

[43] Hashim, N., Sharif, S.N.M., Muda, Z., Isa, I.M., Ali, N.M., Bakar, S.A., Sidik, S.M., Hussein, M.Z., Preparation of zinc layered hydroxide-ferulate and coated zinc layered hydroxide-ferulate nanocomposites for controlled release of ferulic acid. *Mater. Res. Innov.*23 (2018) 233–245.

[44] Ghazali, S.A.I.S.M., Hussein, M.Z., Sarijo, S.H., 3,4-Dichlorophenoxyacetate interleaved into anionic clay for controlled release formulation of a new environmentally friendly agrochemical. *Nanoscale Res. Lett.*8 (2013) 1–8.

[45] Li, S., Shen, Y., Xiao, M., Liu, D., Fan, L., Synthesis and controlled release properties of β-naphthoxyacetic acid intercalated Mg–Al layered double hydroxides nanohybrids. *Arab. J. Chem.*12 (2015) 2563–2571.

[46] Sarijo, S.H., Ghazali, S.A.I.S.M., Hussein, M.Z., Ahmad, A.H., Intercalation, physicochemical and controlled release studies of organic-inorganic–herbicide (2,4,5 tricholorphenoxy butyric acid) nanohybrid into hydrotalcite-like compounds. *Mater. Today Proc.*2 (2015) 345–354.

[47] Ghori, M.U., Conway, B.R., Hydrophilic matrices for oral control drug delivery. *Am. J. Pharmacol. Sci.*3 (2015) 103–109.

[48] Serrano-Cruz, M.R., Villanueva-Carvajal, A., Morales Rosales, E.J., Ramírez Dávila, J.F., Dominguez-Lopez, A., Controlled release and antioxidant activity of Roselle (Hibiscus sabdariffa L.) extract encapsulated in mixtures of carboxymethyl cellulose, whey protein, and pectin. *LWT-Food Sci. Technol.*50 (2013) 554–561.

[49] Cozzolino, C.A., Nilsson, F., Iotti, M., Sacchi, B., Piga, A., Farris, S., Exploiting the nano-sized features of microfibrillated cellulose (MFC) for the development of controlled-release packaging. *Colloids Surf. B Biointerfaces*110 (2013) 208–216.

[50] Hussein, M.Z., Rahman, N.S.S.A., Sarijo, S.H., Zainal, Z., Synthesis of a monophasic nanohybrid for a controlled release formulation of two active agents simultaneously. *Appl. Clay Sci.*58 (2012) 60–66.

[51] Ho, Y.S., Mckay, G., Pseudo-second order model for sorption processes. *Process Biochem.*34 (1999) 451–465.

[52] Kodama, T., Harada, Y., Ueda, M., Shimizu, K.I., Shuto, K., Komarneni, S., Selective exchange and fixation of strontium ions with ultrafine Na-4-mica. *Langmuir*17 (2001) 4881–4886.

[53] Ritger, P.L., Peppas, N.A., A simple equation for description of solute release II. Fickian and anomalous release from swellable devices. *J. Control. Release*5 (1987) 37–42.

[54] Woo, M.A., Woo Kim, T., Paek, M.-J.J., Ha, H.-W.W., Choy, J.-H.H., Hwang, S.-J.J., Kim, T.W., Paek, M.-J.J., Ha, H.-W.W., Choy, J.-H.H., Hwang, S.-J.J., Phosphate-intercalated CaFe-layered double hydroxides: crystal structure, bonding character, and release kinetics of phosphate. *J. Solid State Chem.*184 (2011) 171–176.

[55] Hashim, N., Muda, Z., Hamid, S.A., Isa, I.M., Kamari, A., Mohamed, A., Hussein, M.Z., Ghani, S.A., Characterization and controlled release formulation of agrochemical herbicides based on zinc-layered hydroxide-3-(4-methoxyphenyl) propionate nanocomposite. *J. Phys. Chem. Sci.*1 (2014) 1–6.